Hindawi
Modelling and Simulation in Engineering
Volume 2019, Article ID 8384051, 10 pages
https://doi.org/10.1155/2019/8384051

Research Article

Hydration of Early Age Cement Paste with Nano-$CaCO_3$ and SAP by LF-NMR Spectroscopy: Mechanism and Prediction

Haitao Zhao,[1] **Gaoyang Sun**,[2] **Lu Yu**,[3] **Kaidi Jiang**,[4] **Xiaodong Chen**,[5] **Ruiming Jia**,[6] **Yi Wan**,[7] **and Shihai Li**[8]

[1]*College of Materials Science and Engineering, Southeast University, Nanjing 211189, China*
[2]*Jiangsu Testing Center for Quality of Construction Engineering Co. Ltd., Nanjing 210028, China*
[3]*Nanjing Architectural Design & Research Institute Co. Ltd., Nanjing 210005, China*
[4]*College of Civil and Transportation Engineering, Hohai University, Nanjing 210098, China*
[5]*China Communications Construction Company Urban Investment Holding Co. Ltd., Guangzhou 510623, China*
[6]*Tong Yuan Design Group Co. Ltd., Jinan 250101, China*
[7]*Anhui Transport Consulting & Design Institute Co., Ltd., Hefei 230088, China*
[8]*Dalian Luneng Real Estate Co. Ltd., Dalian 116000, China*

Correspondence should be addressed to Haitao Zhao; hhuzhaoht@163.com

Received 20 June 2019; Accepted 25 July 2019; Published 14 August 2019

Guest Editor: Qing-feng Liu

Copyright © 2019 Haitao Zhao et al. This is an open access article distributed under the Creative Commons Attribution License, which permits unrestricted use, distribution, and reproduction in any medium, provided the original work is properly cited.

In this paper, by testing the evolution of the physically bound water using the low-field nuclear magnetic resonance (LF-NMR) technology, the hydration process of cement paste with nano-$CaCO_3$ (NC) and superabsorbent polymer (SAP) at early age is investigated. Results indicate that the hydration process can be divided into four periods according to the zero points of the second-order differential hydration curve: initial period, acceleration period, deceleration period, and steady period. Firstly, with the increase in the water to cement ratio, the starting time of the hydration period is delayed, and the duration becomes longer. Secondly, the addition of NC leads to the speedy arrival of each period and shortens the duration of each period in the hydration process, and the optimal NC content is 1.5%. Thirdly, with the increase in SAP content, the starting time of the hydration period is delayed and the duration becomes longer. Finally, based on the experimental results and the existing hydration model, the modified hydration model considering the content of NC and SAP is proposed.

1. Introduction

Concrete is the most widely used man-made construction material in the world, and the mechanical property and durability are focused in recent studies [1–5]. Nanomaterials, as products of nanotechnology, are defined as materials with particle sizes less than 100 nm and have many superior properties that differ from traditional materials [6, 7]. Nanomaterials can enhance the physical and mechanical properties of the cement-based materials effectively, reduce the porosity, and help in manufacturing the concrete with better performance [8]. The price of nano-SiO_2 [9], nano-Al_2O_3 [10], nano-TiO_2 [11], and other materials are very expensive, which makes it difficult to be widely used in cement-based materials. But NC has many advantages such as low price, small particle size, and large surface area, which can be filled with cement particles to make the microstructure more compact [12]. The research indicates that NC can promote hydration process and induce new hydration products [13]. Therefore, it is significant to study the effect of NC on the hydration process of cement-based materials. Furthermore, traditional external curing methods are not effective because the curing water penetrates only the surface layer of the concrete [14]. Internal curing with SAP is an effective method to reduce the decrease in internal relative humidity by supplying additional water [15] and to prevent the detrimental effects of shrinkage by producing a dense crack-free microstructure [16].

Scholars have done a series of experimental studies on the influence of NC or SAP on cement-based materials. Wang and Zhang [17] studied the effects of NC on the hydration properties of silicate cement by using the microthermograph method and the differential scanning thermal analysis. The results showed that the use of NC could promote the hydration and enhance the heat of hydration. Liu et al. [18] used the ultrasonic method to study the influence of NC on the performance of cement paste. The results showed that when the dosage of NC was 2%, the initial time and final time of concrete were shortened by 61 min and 39 min, respectively. So, the addition of NC can promote the hydration reaction of cement paste. Camiletti et al. [19] studied the effect of NC on the performance of super-high-performance concrete by using thermal analysis. The results indicated that NC accelerates the hydration process of cement by inducing nucleation effect. Esteves [20] studied the hydration degree of cement paste and mortar by using the differential thermogravimetric analysis. The results showed that SAP promoted cement hydration. Justs et al. [21] found that SAP promoted hydration of cement-based materials from 7 to 28 days. However, there is no research on the combined impact of NS and SAP on hydration of cement-based materials at present. Thus, the effects of NC and SAP on the hydration process of cement-based materials were investigated in this paper.

At present, there are many research methods of the early age hydration process such as ultrasonic method [22], resistivity method [23], hydrated thermal analysis method [24], and ultrasonic testing method [25]. These methods have made great progress in the study of hydration process. However, there are still many deep-seated mechanisms that have not been systematically solved, especially the interaction among various mineral hydration. Low-field nuclear magnetic resonance (LF-NMR) technology is utilized to study the hydration of cement-based materials by testing the evolution of the physically bound water [26, 27]. It is quick, continuous, and lossless. Apih et al. [28] found that the longitudinal relaxation time (T_1) of the cement paste decreased with the progress of hydration, which could reveal the different periods of cement hydration. She et al. [29] measured the T_2 signal intensity of the physically bound water in the cement paste and found that the evolution of T_2 could well describe the hydration kinetics. The initial period, acceleration period, and steady period were characterized according to the different rates of change. Moreover, the reaction and the mechanism of each period were discussed based on the theory of cement chemistry.

In this paper, the effects of the water to cement ratio (w/c), NC, and SAP on the hydration process of cement paste are tested and discussed based on LF-NMR. Furthermore, the modified hydration model considering the effects of NC and SAP is proposed.

2. Materials and Methods

2.1. Materials. In this experiment, P.II52.5 Portland cement with the specific surface area of 350 m^2/kg and density of 3180 kg/m^3 was used. The chemical composition of cement is shown in Table 1. NC (Figure 1) with the purity of the NC of above 95 wt.% and grain size ranging from 40 nm to 80 nm was used in this test. The polycarboxylic high-performance water-reducing agent produced by Sobute New Materials Company Ltd. (Nanjing, China) was used. However, the SAP (Figure 2) used in this study is an organic-inorganic polymer material and the water absorption capacity is 20 g water per gram of SAPs.

The influencing factors of the hydration are selected as w/c, NC content, and SAP content. The NC content is 1.0%, 1.5%, 2.0%, and 3.0% replacing the cement by weight. The dosage of SAP is 0.15% and 0.30% by mass of cement, and the w/c ratios are 0.30, 0.35, and 0.40. Furthermore, nine different cement compositions are designed (Table 2), and the time of each test is 96 hours.

In Table 2, SJ indicates that the cementitious material in the sample consists of cement only, and NC indicates that the cementitious material in the sample consists of cement and NC. For example, 0.30SJ_NC015S15 represents a sample with a w/b value of 0.30, an NC content of 1.5%, and an SAP content of 0.15%.

2.2. Specimen Preparation. Cement paste specimens were mixed using a paddle mixer following a procedure which was similar to ASTM C-305 [30] as follows.

Cement and water and the admixture if necessary were weighed; sometimes one kind of particular admixture was added to water in a bowl. The mixture was initially mixed at 140 revolutions per minute (rpm) for 30 seconds. Taking a pause for 1 minute, meanwhile cement paste adhering to the sides of the mixing bowl was scraped. The entire mixture was mixed for another 2.5 minutes at 285 rpm. Then, the cement paste was cast into a glass tube with a height of 200 mm and a diameter of 27 mm until the height of samples were approximately 20–30 mm and then sealed with plastic film immediately after pouring.

2.3. Testing Methods. All of the experiments were carried out on a PQ001 LF-NMR with a magnetic field of 0.42 T and proton frequency field of 18 MHz. The room temperature was held constant at $20 \pm 1^{\circ}$C.

Before the test, the free induction decay (FID) sequence was calibrated on the oil sample to obtain the offset of RF signal frequency (O1) and the width of $\pi/2$ pulse (P1). Then Carr-Purcell-Meiboom-Gill (CPMG) sequence ($\pi/2$-(τ-π-τ) n-TR) was applied to measure the transverse relaxation time T_2 of pastes. $\pi/2$ and π were pulses which could rotate the magnetization vector about the axis where pulses were applied. TR was the waiting time between two measurements, and n was the number of sampling data. The parameter settings for LF-NMR are given in Table 3.

By monitoring the T_2 signal of physically bound water in cement paste using LF-NMR, the wave crest amplitude of the T_2 signal, $A(t)$, is used to characterize the hydration process, as shown in Figure 3(a). Then the curve about $A(t)$ in the unit mass of cement paste and different hydration time are obtained (Figure 3(b)). According to the zero point (b_1, b_2, and b_3) of the second-order differential curve (Figure 3(c)), the hydration process can be divided into four periods: initial period, acceleration period, deceleration period, and steady period, as shown in Figure 3(b).

Table 1: Chemical composition of cement.

Material	SiO_2	Al_2O_3	Fe_2O_3	CaO	MgO	Na_2O	K_2O	SO_3	TiO_2	LOI
Cement	19.53	4.31	2.89	63.84	1.25	0.13	0.64	3.25	0.26	3.0

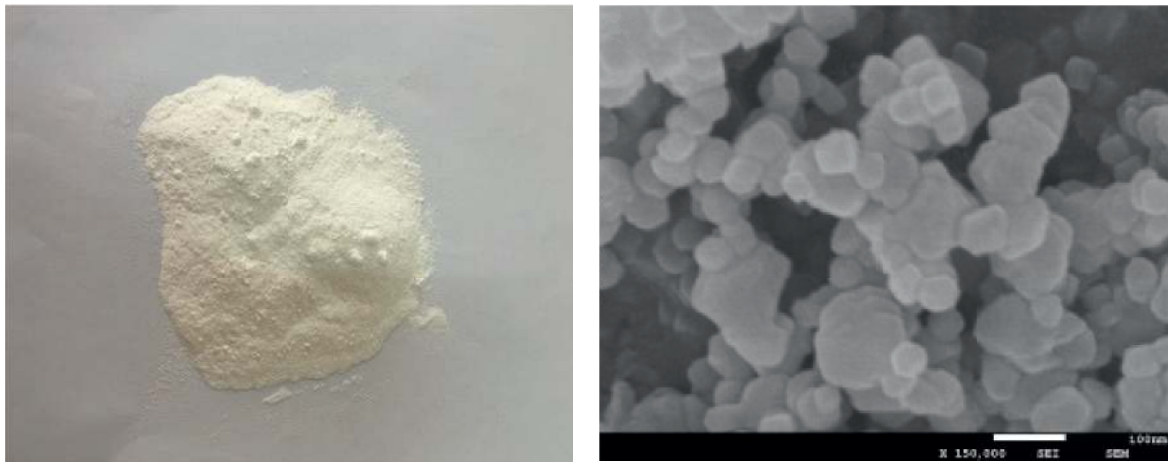

(a) (b)

Figure 1: NC diagram. (a) NC powder. (b) SEM image of NC.

Figure 2: SAP.

3. Results and Discussion

3.1. Effect of w/c on the Hydration Process. Figure 4 shows the curves of T_2 signal amplitude in unit mass with different w/c. The larger the w/c is, the more physically bound water in the unit mass of cement paste contains. According to the method introduced above, the test data are treated as differential treatment, and then the time cutoff point of the four periods is obtained. The results are shown in Figure 4 and Table 4.

It can be seen from Figure 4 that the unit signal amplitude of three cement pastes decreases with age. In the early stage of the initial phase, C_3A (tricalcium aluminate), the most active in cement, has begun to react with water. And the hydrated product is encapsulated on the cement surface to form a gel protective film. In the later stage of the initial phase, the gel protective layer like the permeable membrane only allows water molecules to enter the protective layer. But it does not allow Ca^{2+} and OH^- ions to go through the protective layer. Further progress of the hydration reaction is prevented. At the end of the initial phase, the T_2 signal amplitude of the samples 0.30SJ, 0.35SJ, and 0.40SJ decreases to 471.3 a.u./g, 649.3 a.u./g, and 805.6 a.u./g, respectively. At any time of this stage, the T_2 signal amplitude in unit mass increases as the w/c increases. The reason is that the greater the w/c, the more the water contained in the per unit mass of cement paste, and the greater the detection of physically bound water signal.

The duration of the initial period of the samples 0.30SJ, 0.35SJ, and 0.40SJ is 1.65 h, 1.872 h, and 2.033 h, respectively. The larger the w/c is, the longer the initial period is. The reason is perhaps that the larger the w/c, the lower the Ca^{2+} concentration in the solution, which increases the degree of cement hydration. Furthermore, larger w/c delays Ca^{2+} to reach the time of super saturation, prolonging the initial period. At the end of the initial period, the protective layer of the gel layer produced in the previous stage ruptures due to the change in permeability. The new cement surface comes into contact with water, and the acceleration period begins.

At the acceleration stage, Ca^{2+} achieves super saturation, which makes Ca^{2+} crystal to precipitate and promotes the hydration of C_3S (tricalcium silicate). Water is rapidly consumed, and the signal quantity decreases quickly. At the end of the acceleration period, the T_2 signal amplitude of the samples 0.30SJ, 0.35SJ, and 0.40SJ decreases to 402.3 a.u./g, 564.7 a.u./g, and 705.3 a.u./g, respectively. The decreasing rates are 21.1 a.u./g/h, 24.5 a.u./g/h, and 27.5 a.u./g/h, respectively. It indicates that the larger the w/c is, the faster the hydration rate is.

At the end of the acceleration period, the hydration product has been produced in large quantity. The hydration products have been accumulated and formed on the outer shell of the protective layer. These shells are connected to each other to form a mesh structure. The T_2 signal amplitude of the samples 0.30SJ, 0.35SJ, and 0.40SJ reduces to 162.3 a.u./g, 277.0 a.u./g, and

Table 2: Mix proportion of cement pastes.

Sample	w/b	Dosage of NC (%)	Dosage of SAP (%)	Influencing factor
0.30SJ	0.30	0	0	w/c
0.35SJ	0.35	0	0	
0.40SJ	0.40	0	0	
0.30SJ_NC010	0.30	1.0	0	NC content
0.30SJ_NC015	0.30	1.5	0	
0.30SJ_NC020	0.30	2.0	0	
0.30SJ_NC030	0.30	3.0	0	
0.30SJ_NC015S15	0.30	1.5	0.15	SAP content
0.30SJ_NC015S30	0.30	1.5	0.30	

Table 3: Parameter settings for LF-NMR.

Sequence	TD	SW	RFD	RG1	DRG1	PRG	TW	NS	NECH	TE	DL1
FID	1024	100	0.02	20	3	2	2000	4	—	—	—
CPMG	Automatic settings	250	0.005	10	3	2	200	16	500	0.11	500

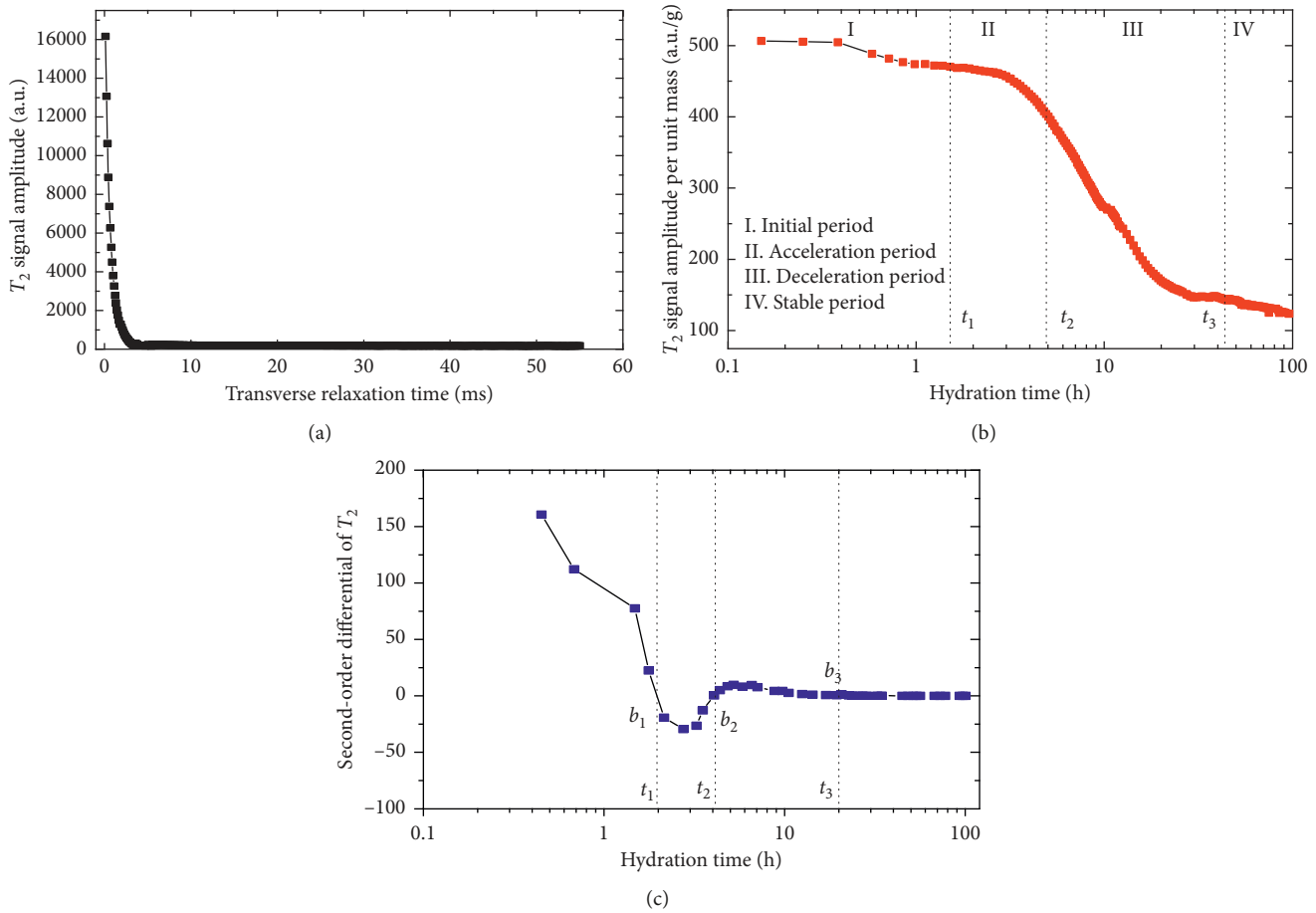

Figure 3: Schematic diagram of hydration process. (a) First wave crest amplitude of (T_2) signal. (b) The first peak amplitude $A(t)$ in unit mass changes with time. (c) Second-order differential of $A(t)$.

371.1 a.u./g, respectively. The reason is that the larger the w/c, the more the water contained in the cement gap and pore diameter in the cement paste, and the more the presence of physically bound water.

At the end of the deceleration period, the T_2 signal amplitude of the samples 0.30SJ, 0.35SJ, and 0.40SJ decreases to 124.7 a.u./g, 203.2 a.u./g, and 266.3 a.u./g, respectively. The T_2 signal amplitude in unit mass is very small and tends to be stable, and the rate of hydration process is very slow. The time of the steady period of the samples 0.30SJ, 0.35SJ, and 0.40SJ is 50.583 h, 52.815 h, and 54.117 h, respectively. The larger the w/c, the longer the time requires to reach the steady period.

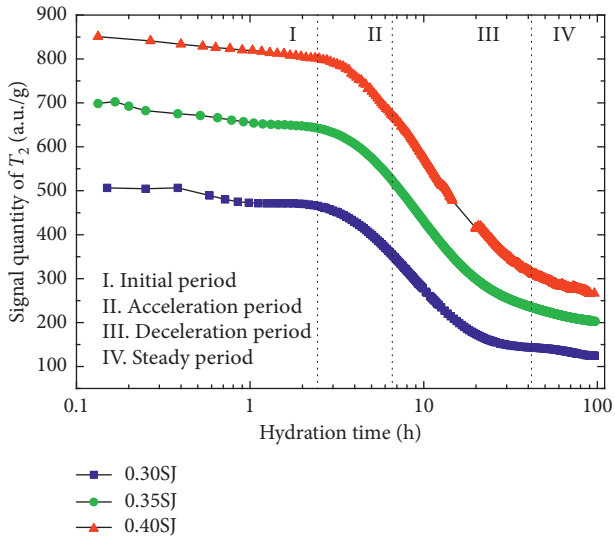

Figure 4: Effects of different w/c on the hydration process.

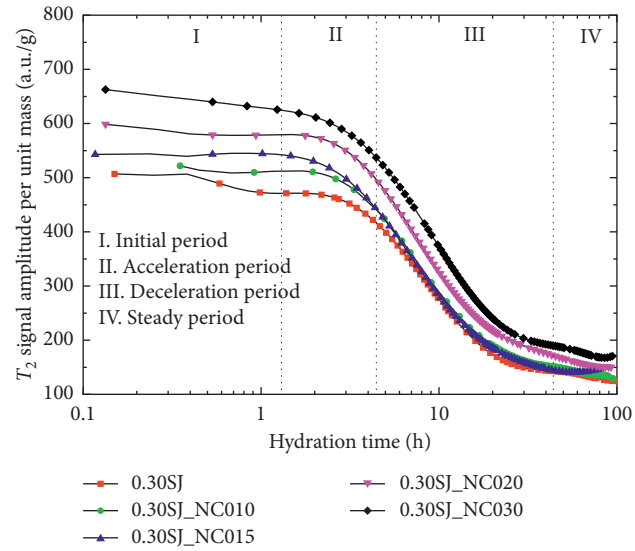

Figure 5: Effects of different NC dosages on the hydration process.

Table 4: The hydration period separation time of pure cement pastes with different w/c.

Sample	t_1 (h)	t_2 (h)	t_3 (h)	(0~t_1)	(t_2~t_3)	(t_3~)
0.30NC0	1.65	4.977	50.583	1.65	3.327	45.606
0.35NC0	1.872	5.324	52.815	1.517	3.452	47.491
0.40NC0	2.033	5.677	54.117	0.867	3.644	48.44

3.2. Effect of NC on the Hydration Process. The curves of T_2 signal amplitude in unit mass of cement paste with an NC dosage of 0%, 1.0%, 1.5%, 2.0%, and 3.0% with hydration time are shown in Figure 5. According to the same division method of the hydration process abovementioned, the hydration process is divided into four periods, and each period duration is listed in Table 5. For cement paste with same w/c, the addition of NC makes the T_2 signal amplitude in unit mass stronger. As binder materials continuously hydrate, T_2 signal amplitude in all samples is on the decline with different rates. But different dosages of NC have an obviously distinct influence on each period.

It can be observed in Figure 5 that with the increase of NC content, the T_2 signal amplitude gradually increases, and the increase rate is not proportional. At the beginning of the initial period, the T_2 signal amplitude of the samples 0.30SJ, 0.30SJ_NC010, 0.30SJ_NC015, 0.30SJ_NC020, and 0.30SJ_NC030 is 506.78 a.u./g, 521.95 a.u./g, 542.92 a.u./g, 598.71 a.u./g, and 662.52 a.u./g, respectively. Compared with the baseline group, the T_2 signal amplitude of NC cement paste increases 15.17 a.u./g, 36.14 a.u./g, 91.93 a.u./g, and 155.74 a.u./g, respectively. And the corresponding growth rates are 3.0%, 7.13%, 18.14%, and 30.73%, respectively. There is no corresponding linear relationship. NC particle size ranges from 40 nm to 80 nm, which can be filled in small pores to function as microaggregates, so that the relative content of water in the pores is reduced and the free water of the surface involved in the reaction relatively increases. When the amount of NC is increased, more porous pores are filled and more free surface water content exists.

Table 5: The hydration period separation time of cement pastes with different NC dosages.

Sample	t_1 (h)	t_2 (h)	t_3 (h)	(0~t_1)	(t_2~t_3)	(t_3~)
0.3NC0	1.65	4.977	50.583	1.65	3.327	45.606
0.3NC1.0	1.517	4.817	48.8	1.517	3.3	43.983
0.3NC1.5	1.167	4.317	42.117	1.167	3.15	37.8
0.3NC2.0	1.342	4.587	46.357	1.342	3.245	41.77
0.3NC3.0	1.233	4.465	45.516	1.233	3.232	41.051

It can obviously be seen in Table 5 that during the hydration process, with the addition of NC, the duration of four stages are all shortened. When the NC content is 1.5%, the starting time of each hydration period is the earliest and thus the duration of each period is the shortest. Therefore, the addition of NC can promote the hydration process of cement paste, and the optimal NC content is 1.5%. The conclusion is similar with the previous study of hydration process [31]. The duration of the initial period of the samples 0.30SJ, 0.30SJ_NC010, 0.30SJ_NC015, 0.30SJ_NC020, and 0.30SJ_NC030 is 1.65 h, 1.517 h, 1.167 h, 1.342 h, and 1.233 h, respectively. At the beginning of the acceleration period, the T_2 signal amplitude of the samples 0.30SJ, 0.30SJ_NC010, 0.30SJ_NC015, 0.30SJ_NC020, and 0.30SJ_NC030 is 471.31 a.u./g, 512.51 a.u./g, 545 a.u./g, 579.55 a.u./g, and 625.60 a.u./g, respectively. At the end of the acceleration period, the T_2 signal amplitude is 402.31 a.u./g, 431.83 a.u./g, 444.8 a.u./g, 491.57 a.u./g, and 537.18 a.u./g, respectively.

There are several reasons for abovementioned phenomenon [32]. Firstly, the particle size of NC is in nanometer, and its strong surface activity can change the distribution of cement particles. The microaggregate effect can increase the relative content of free water so as to increase the contact area between cement particles and water. Secondly, NC makes the diffused Ca^{2+} to accumulate on its particle surface, decreasing the nearby Ca^{2+} concentration and accelerating the chemical reaction of C_3S, which promotes the hydration process. Thirdly, NC has a high

chemical activity to increase the distribution of cement particles, increasing the contact area between water and cement particles. Finally, when NC contacts C_3A, a small amount of calcium aluminate ($CaCO_3{\cdot}C_3A{\cdot}H_2O$) is be produced. It can make water molecules and other particles spread so as to accelerate the hydration process. However, when the content of NC is over 1.5%, the phenomenon of "bleeding" may occur and the active influence on the hydration process falls. So, the optimal NC content is 1.5%.

3.3. Effect of SAP on the Hydration Process. The curves of the T_2 signal amplitude of cement paste with different SAP content are presented in Figure 6. According to the same division method introduced above, each period's duration is shown in Table 6.

It can be seen from Figure 6 that, in the four stages of hydration process, with the increase of SAP content, the T_2 signal amplitude gradually increases. At the end of the initial period, the T_2 signal amplitude of the samples 0.30SJ_NC015, 0.30SJ_NC015S15, and 0.30SJ_NC015S30 is 534.022 a.u./g, 698.244 a.u./g, and 756.576 a.u./g, respectively. The pre-absorbent of water in SAP introduces extra water, which releases moisture due to the concentration difference and self-drying. Thus, the amount of physical bound water is greater.

It can be observed in Table 6 that, with the increase in SAP content, the starting time of each hydration period is also delayed and thus the duration of each period is prolonged. The starting time of the deceleration period of the samples 0.30SJ_NC015, 0.30SJ_NC015S15 and 0.30SJ_NC015S30 is 4.317 h, 4.433 h, and 4.583 h, respectively. Thus, the duration is 42.117 h, 43.067 h, and 43.3 h, respectively. SAP continuously releases moisture to promote the hydration process [33]. It makes the total w/c larger. With the proceeding of hydration, the relative concentration of Ca^{2+} per unit volume decreases, and the time to reach the saturation state prolongs.

In addition, it can obviously be seen from Figure 6 that the T_2 signal amplitude of NC cement paste mixed with SAP continued to decline at the steady period. However, the T_2 signal amplitude without SAP is almost constant. Taking hydration time from 82 h to 96 h, for example, the T_2 signal amplitude of the samples 0.30SJ_NC015, 0.30SJ_NC015S15, and 0.30SJ_NC015S30 is 0.347 a.u./g, 7.782 a.u./g, and 6.353 a.u./g. The descending rates are 0.025 a.u./g/h, 0.556 a.u./g/h, and 0.454 a.u./g/h. With the proceeding of hydration, the free water in the cement paste is continuously consumed. SAP gradually releases moisture due to poor concentration of capillary solution, humidity difference, and capillary tensile stress [28]. The results are consistent with previous studies [34].

3.4. Hydration Model

3.4.1. Hydration Model for Pure Cement Paste. The hydration model can be used to describe and predict the development of hydration. The Avrami–Erofeev equation [35] is the classic overall kinetic equation and has many significant advantages, such as a more simplified expression and less parameters. The Avrami–Erofeev equation is as follows:

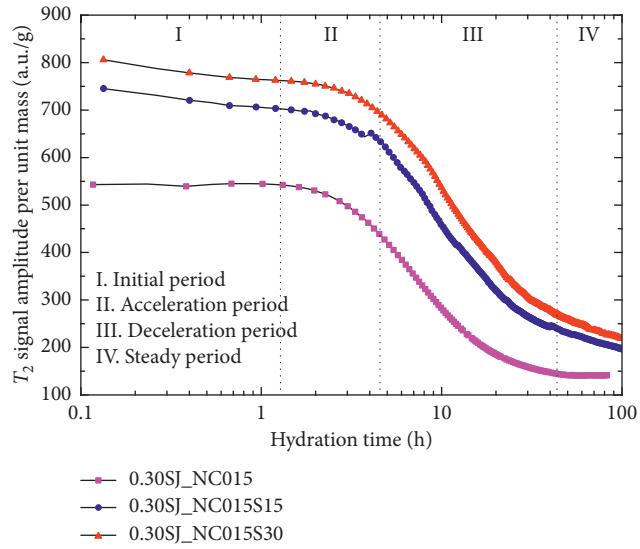

Figure 6: Effects of different SAP dosages on the hydration process.

Table 6: The hydration period separation time of cement pastes with different SAP dosages.

Sample	t_1 (h)	t_2 (h)	t_3 (h)	(0~t_1)	(t_2~t_3)	(t_3~)
0.3NC1.5	1.167	4.317	42.117	1.167	3.15	37.8
0.3NC1.5S0.15	1.233	4.433	43.067	1.233	3.2	38.634
0.3NC1.5S0.3	1.367	4.583	43.3	1.367	3.216	38.717

$$\alpha(t) = 1 - \exp\left(-(kt)^n\right), \tag{1}$$

where $\alpha(t)$ is the degree of hydration, k and n are the empirical parameters, and t is the time of cement paste hydration.

On the basis of this model, the variation law of T_2 with time is described. And the hydration process is characterized by transverse relaxation time. The expression of the T_2 signal amplitude over time is as follows:

$$T(t) = a - b\exp(-ct), \tag{2}$$

where $T(t)$ is the T_2 signal amplitude of unit mass of cement paste hydration at t moment and a, b, and c are the model parameters, which depend on mineral compositions, w/c, etc.

The experiment data and fitting curves of pure cement pastes with different w/c are given in Figure 7. The fitted results including fitting parameters and correlation are listed in Table 7.

$$\begin{aligned} a &= 561.71 - 2716.32\ln(\mathrm{w/c}) - \frac{1110.51}{w/c}, \\ b &= -3140.24 + 11138.79(\mathrm{w/c})^3 + \frac{727.71}{(\mathrm{w/c})}, \\ c &= 0.22 - 0.38\ln(\mathrm{w/c}) - \frac{0.32}{(\mathrm{w/c})^{0.5}}, \end{aligned} \tag{3}$$

where the w/c ranges from 0.3 to 0.4 and the hydration time t ranges from 0 h to 110 h.

As presented in Table 7, the correlation of experiment data and fitting curves is all over 0.99, and equation (2) could

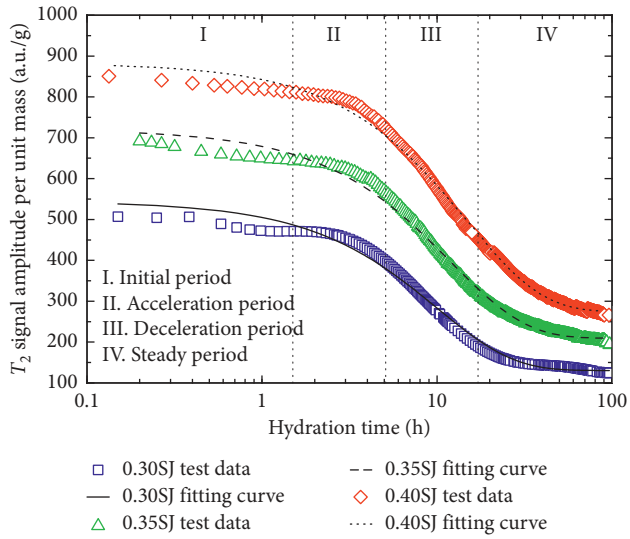

Figure 7: Experiment data and fitting curves of pure cement pastes with different w/c.

Table 7: Fitting parameters and correlation of pure cement pastes with different w/c.

Sample	a	b	c	Correlation
0.3NC0	130.385	−413.786	0.0996	0.9975
0.35NC0	240.477	−583.487	0.0840	0.9972
0.4NC0	274.374	−608.077	0.0679	0.9983

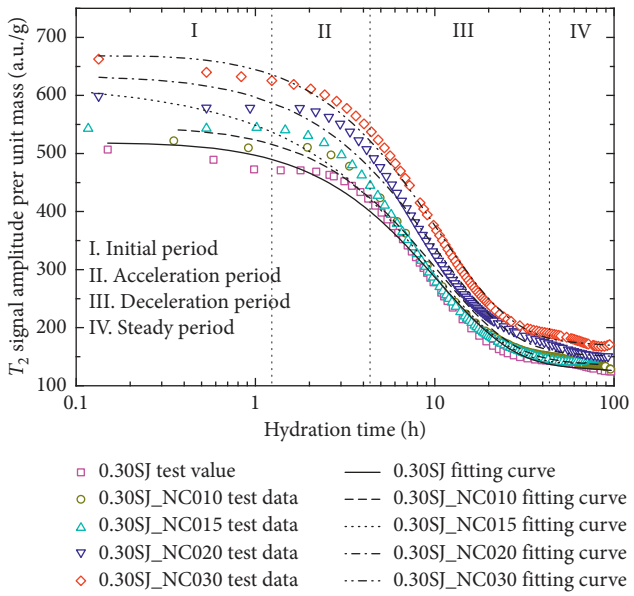

Figure 8: Experiment data and fitting curves of cement pastes with different NC dosages.

describe the hydration process of pure cement pastes very well. According to Table 7, the relations of a, b, and c with w/c are proposed by regression analysis.

3.4.2. Modification of Hydration Model. The hydration model above only describes the hydration process of the neat cement paste. The effect of NC and SAP on the hydration process of cement paste is not mentioned. Through the hydration model obtained in Section 3.4.1, it can be found that it has the advantages such as simple expression, few parameters, and simple calculation. Therefore, this section modifies the hydration model based on the Avrami–Erofeev model. The expression is as follows:

$$T(t) = \gamma_{SAP}\gamma_{NC}[a - b\exp(-ct)], \quad (4)$$

Table 8: Fitting parameters and correlation of cement pastes with different NC dosages.

Sample	A_{NC}	B_{NC}	C_{NC}	Correlation
0.3NC0	0.911	−0.0011	0.075	0.9955
0.3NC1.0	0.945	−0.0014	0.093	0.9929
0.3NC1.5	1.195	0.0017	−0.111	0.9907
0.3NC2.0	1.1479	−0.0007	0.036	0.9895
0.3NC3.0	1.1601	−0.0014	0.118	0.9946

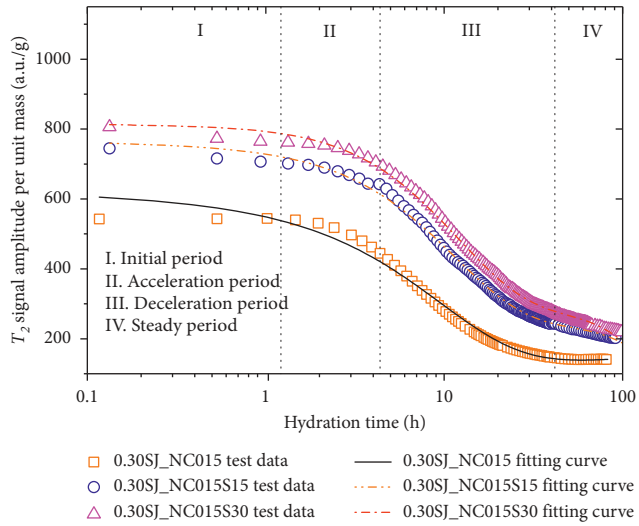

Figure 9: Experiment data and fitting curves of cement pastes with different SAP dosages.

where γ_{NC} and γ_{SAP} are the parameters which are related to the dosage of NC and SAP.

The experiment data and fitting curves of cement pastes with different NC dosages are shown in Figure 8. The fitted results including fitting parameters and correlation are listed in Table 8.

As presented in Table 8, the correlation of experiment data and fitting curves is all over 0.99, and equation (4) could well describe the hydration process of cement pastes with different NC dosages. According to Table 8, the relations of A_{NC}, B_{NC}, and C_{NC} with NC content (M_{NC}) are proposed by regression analysis:

$$\begin{aligned}
\gamma_{NC} &= A_{NC} + B_{NC}t + C_{NC}t^{0.19},\\
A_{NC} &= \frac{m_{NC}}{m_{NC} - 0.935} - \frac{0.857}{m_{NC} - 0.941} + 0.04m_{NC},\\
B_{NC} &= \frac{8.722m_{NC} - 0.001}{m_{NC} - 1.45},\\
C_{NC} &= \frac{0.07 - 0.02m_{NC}^2}{1 - 0.58m_{NC}^2 + 0.036m_{NC}^4},
\end{aligned} \tag{5}$$

where the NC content m_{NC} ranges from 0.01 to 0.03% and the hydration time t ranges from 0 h to 110 h.

The experimental data and fitting curves of cement pastes with different SAP dosages are shown in Figure 9. The fitted results including fitting parameters and correlation are listed in Table 9.

Table 9: Fitting parameters and correlation of cement pastes with different SAP dosages.

Sample	A_{SAP}	B_{SAP}	C_{SAP}	γ_{SAP}	Correlation
0.3NC1.5	1.017	−0.032	0.115	1.0572	0.994
0.3NC1.5S0.15	1.236	−0.042	0.135	1.0572	0.998
0.3NC1.5NC0.3	1.312	−0.062	0.196	1.0572	0.998

As presented in Table 8, the correlation of experiment data and fitting curves is all over 0.99 and the equation (4) could well describe the hydration process of cement pastes with different SAP dosages. According to Table 9, the relations of A_{SAP}, B_{SAP}, and C_{SAP} with SAP content (m_{SAP}) are proposed by regression analysis:

$$\begin{aligned}
\gamma_{SAP} &= A_{SAP} + B_{SAP}t + C_{SAP}t^{0.75},\\
A_{SAP} &= 3.84 - 1.68m - 2.73\exp(-m_{SAP}),\\
B_{SAP} &= 0.02 - 0.43m^3 - 0.053\exp(m_{SAP}),\\
C_{SAP} &= -0.07 + 0.78m^{1.5} + 0.18\exp(-m_{SAP}),
\end{aligned} \tag{6}$$

where the SAP content m_{SAP} ranges from 0 to 0.3% and the hydration time t ranges from 0 h to 110 h.

4. Conclusions

From the materials and measurement methods used in this study, the following conclusions can be drawn:

(1) With the development of hydration reaction, T_2 signal amplitude in unit mass of different cement pastes always decreases with age, and the hydration process of the cement paste can be divided into four periods according to the second-order differential zero point of the curve: initial period, acceleration period, deceleration period, and steady period. The larger the w/c is, the greater the T_2 signal amplitude in unit mass is. And the increase of the w/c delays the arrival of the acceleration period, deceleration period, and steady period, and hence, the periods of initial, acceleration, and deceleration last longer.

(2) With the addition of NC in the cement paste, the T_2 signal amplitude increases, the arrival of each period is faster, and hence, the duration of each period becomes shorter. When the content of NC exceeds 1.5%, the effect of promoting the hydration process is weakened. So, the optimal content of NC is 1.5%.

(3) The addition of SAP increases the T_2 signal amplitude of the cement paste, and the T_2 signal amplitude increases as the SAP content increases, but the arrival of the acceleration period, deceleration period, and steady period delays, thus prolonging the duration of the initial period, acceleration period, and deceleration period.

(4) Based on the Avrami-Erofeev model, combined with the change in the T_2 signal amplitude with the hydration time, the hydration model considering the NC content and the SAP content is proposed. The results of the model are in good agreement with the experimental data.

Data Availability

The data used to support the findings of this study are available from the corresponding author upon request.

Conflicts of Interest

The authors declare that they have no conflicts of interest.

Acknowledgments

The authors gratefully acknowledge the financial supports from the Jiangsu Planned Projects for Postdoctoral Research Funds under Grant no. 1501013C.

References

[1] W. Qiang, W. Dengquan, and C. Honghui, "The role of fly ash microsphere in the microstructure and macroscopic properties of high-strength concrete," *Cement and Concrete Composites*, vol. 83, pp. 125–137, 2017.

[2] Q.-F. Liu, G.-L. Feng, J. Xia, J. Yang, and L.-Y. Li, "Ionic transport features in concrete composites containing various shaped aggregates: a numerical study," *Composite Structures*, vol. 183, pp. 371–380, 2018.

[3] X. H. Shen, Q. F. Liu, Z. Hu, W. Q. Jiang, X. Lin, and D. Hou, "Combine ingress of chloride and carbonation in marine-exposed concrete under unsaturated environment: a numerical study," *Ocean Engineering*, 2019.

[4] L. X. Mao, Z. Hu, J. Xia et al., "Multi-phase modelling of electrochemical rehabilitation for ASR and chloride affected concrete composites," *Composite Structures*, vol. 207, pp. 176–189, 2019.

[5] X. H. Shen, W. Q. Jiang, D. Hou, Z. Hu, J. Yang, and Q. F. Liu, "Numerical study of carbonation and its effect on chloride binding in concrete," *Cement & Concrete Composites*, 2020.

[6] D. Hou, J. Yu, and P. Wang, "Molecular dynamics modeling of the structure, dynamics, energetics and mechanical properties of cement-polymer nanocomposite," *Composites Part B: Engineering*, vol. 162, pp. 433–444, 2019.

[7] W. Li, Z. Huang, F. Cao, Z. Sun, and S. P. Shah, "Effects of nano-silica and nano-limestone on flowability and mechanical properties of ultra-high-performance concrete matrix," *Construction and Building Materials*, vol. 95, pp. 366–374, 2015.

[8] M. S. M. Norhasri, M. S. Hamidah, and A. M. Fadzil, "Morphology and strength of cement paste from clay as nanomaterial," *Applied Mechanics and Materials*, vol. 490-491, pp. 19–24, 2014.

[9] B. W. Jo, C. H. Kim, and J. H. Lim, "Investigations on the development of powder concrete with nano-SiO_2 particles," *KSCE Journal of Civil Engineering*, vol. 11, no. 1, pp. 37–42, 2007.

[10] S. Barbhuiya, S. Mukherjee, and H. Nikraz, "Effects of nano-Al_2O_3 on early-age microstructural properties of cement paste," *Construction and Building Materials*, vol. 52, pp. 189–193, 2014.

[11] L. C. Feng, C. W. Gong, Y. P. Wu, D. C. Feng, and N. Xie, "The study on mechanical properties and microstructure of cement paste with nano-TiO_2," *Advanced Materials Research*, vol. 629, pp. 477–481, 2012.

[12] T. Sato and J. J. Beaudoin, "Effect of nano-$CaCO_3$ on hydration of cement containing supplementary cementitious materials," *Advances in Cement Research*, vol. 23, no. 1, pp. 33–43, 2011.

[13] B. W. Langan, K. Weng, and M. A. Ward, "Effect of silica fume and fly ash on heat of hydration of Portland cement," *Cement and Concrete Research*, vol. 32, no. 7, pp. 1045–1051, 2002.

[14] S. Zhuovsky, K. Kovler, and A. Bentur, "Revisting the protected paste volume concept for internal curing of high-strength concretes," *Cement and Concrete Research*, vol. 41, no. 9, pp. 981–986, 2011.

[15] D. Shen, X. Wang, D. Cheng, J. Zhang, and G. Jiang, "Effect of internal curing with super absorbent polymers on autogenous shrinkage of concrete at early age," *Construction and Building Materials*, vol. 106, pp. 512–522, 2016.

[16] P. Lura, M. Wyrzyykowski, C. Tang, and E. Lehman, "Internal curing with lightweight aggregate produced from biomass-derived waste," *Cement and Concrete Research*, vol. 59, pp. 24–33, 2014.

[17] C. Wang and C. Zhang, "The effect of nano-$CaCO_3$ on the hydration properties of Portland cement," *Silicate Bulletin*, vol. 35, no. 3, pp. 824–830, 2016, in Chinese.

[18] X. Liu, L. Chen, A. Liu, and X. Wang, "Effect of nano-$CaCO_3$ on properties of cement paste," *Energy Procedia*, vol. 16, pp. 991–996, 2012.

[19] J. Camiletti, A. M. Soliman, and M. L. Nehdi, "Effects of nano- and micro-limestone addition on early-age properties of ultra-high-performance concrete," *Materials and Structures*, vol. 46, no. 6, pp. 881–898, 2013.

[20] L. P. Esteves, *Internal curing in cement-based materials*, Ph.D. thesis, Aveiro University, Aveiro, Portugal, 2009.
[21] J. Justs, M. Wyrzykowski, D. Bajare, and P. Lura, "Internal curing by superabsorbent polymers in ultra-high performance concrete," *Cement and Concrete Research*, vol. 76, pp. 82–90, 2015.
[22] G. Trtnik, G. Turk, F. Kavčič, and V. B. Bosiljkov, "Possibilities of using the ultrasonic wave transmission method to estimate initial setting time of cement paste," *Cement and Concrete Research*, vol. 38, no. 11, pp. 1336–1342, 2008.
[23] Z. Bosiljkov and W. Li, "Contactless, traformer-based measurement of the resistivity of materials," pp. 10–28, 2003, US Patent: 6639401.
[24] V. Balek, "The hydration of cement investigated by emanation thermal analysis," *Thermochimica Acta*, vol. 72, no. 1-2, pp. 147–158, 1984.
[25] Ö. K. Keskin, İ. O. Yaman, and M. Tokyay, "Effects of experimental parameters in monitoring the hydration of cement mortars by ultrasonic testing," in *Nondestructive Testing of Materials and Structures*, pp. 437–443, Springer, Dordrecht, Netherlands, 2013.
[26] C. Zhou, F. Ren, Q. Zeng, L. Xiao, and W. Wang, "Pore-size resolved water vapor adsorption kinetics of white cement mortars as viewed from proton NMR relaxation," *Cement and Concrete Research*, vol. 105, pp. 31–43, 2018.
[27] C. Zhou, F. Ren, Z. Wang, W. Chen, and W. Wang, "Why permeability to water is anomalously lower than that to many other fluids for cement-based material?," *Cement and Concrete Research*, vol. 100, pp. 373–384, 2017.
[28] T. Apih, G. Lahajnar, A. Sepe et al., "Proton spin-lattice relaxation study of the hydration of self-stressed expansive cement," *Cement and Concrete Research*, vol. 31, no. 2, pp. 263–269, 2001.
[29] A. She, W. Yao, and Y. Wei, "In-situ monitoring of hydration kinetics of cement pastes by low-field NMR," *Journal of Wuhan University of Technology*, vol. 25, no. 4, pp. 692–695, 2010.
[30] ASTM, *Standard Practice for Mechanical Mixing of Hydraulic Cement Pastes and Mortars of Plastic Consistency*, ASTM, West Conshohocken, PA, USA, 1999.
[31] H. S. Yang, Y. J. Che, and M. Zhang, "Effect of nano-$CaCO_3$/limestone powder composite on the early age cement hydration products," *Key Engineering Materials*, vol. 703, pp. 354–359, 2016.
[32] S. W. M. Supit and F. U. A. Shaikh, "Effect of nano-$CaCO_3$ on compressive strength development of high volume fly ash mortars and concretes," *Journal of Advanced Concrete Technology*, vol. 12, no. 6, pp. 178–186, 2014.
[33] B. Craeye, *Reduction of Autogenous Shrinkage of Concrete by Means of Internal Curing*, Ghent Univerity, Ghent, Belgium, 2006.
[34] L. Dudziak and V. Mechtcherine, "Reducing the cracking potential of ultra-high performance concrete by using super absorbent polymers (SAP)," in *Advances in Cement-Based Materials*, pp. 11–19, CRC Press, Boca Raton, FL, USA, 2010.
[35] K. Van Breugel, *Simulation of Hydration and Formation of Structure in Hardening Cement-Based Materials*, Delft University of Technology, Delft, Netherlands, 1991.

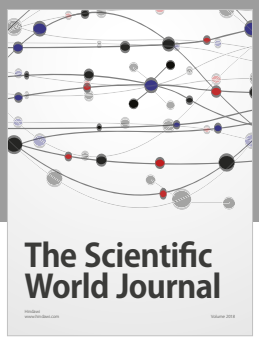

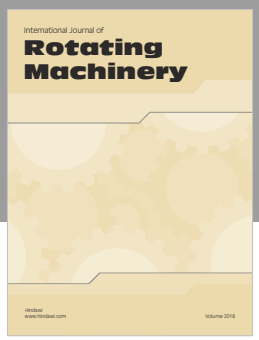

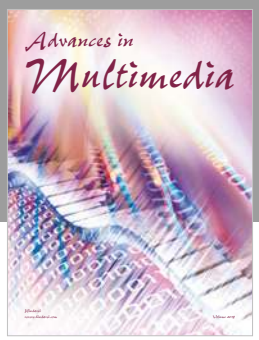

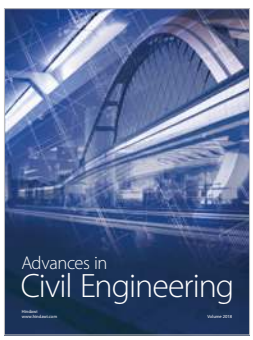

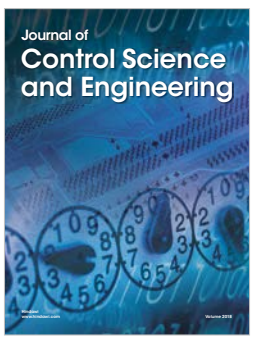

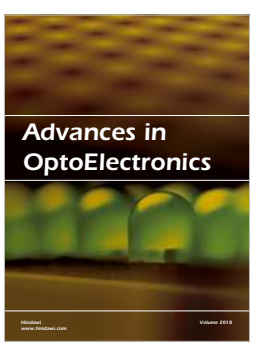

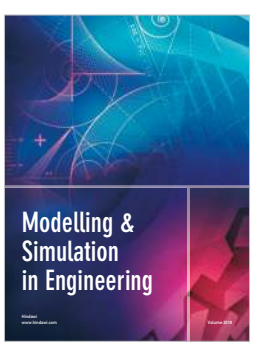

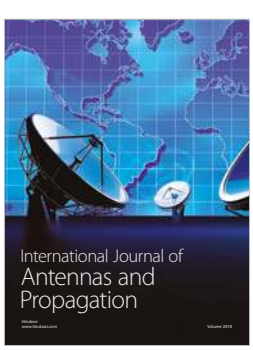

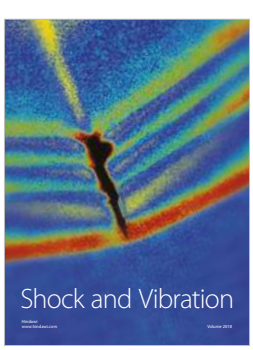

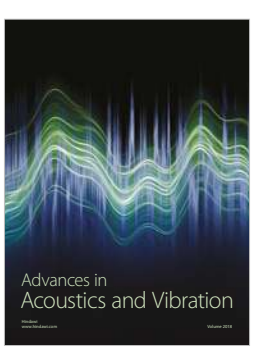

Hindawi

Submit your manuscripts at
www.hindawi.com